



## RESEARCH REPOSITORY

*This is the author's final version of the work, as accepted for publication following peer review but without the publisher's layout or pagination.*

*The definitive version is available at:*

<http://dx.doi.org/10.1038/icb.2016.3>

Thygesen, S.J, Sester, D.P., Cridland, S.O., Wilton, S.D. and Stacey, K.J. (2016) Correcting the NLRP3 inflammasome deficiency in macrophages from autoimmune NZB mice with exon skipping antisense oligonucleotides.

Immunology and Cell Biology, 94 (5). pp. 520-524.

<http://researchrepository.murdoch.edu.au/id/eprint/32009/>

Copyright: © 2016 Australasian Society for Immunology  
It is posted here for your personal use. No further distribution is permitted.

1 **NOTE: this is a pre-refereed version, for which copyright provisions allow archiving.**  
2 **Some figures and information has been altered in the final published version.**

3

4 **This paper is published as:**

5

6 Thygesen SJ, Sester DP, Cridland SO, Wilton SD, **Stacey KJ** (2016) Correcting the NLRP3  
7 inflammasome deficiency in macrophages from autoimmune NZB mice with exon skipping antisense  
8 oligonucleotides. *Immunology and Cell Biology* doi:10.1038/icb.2016.3

9 **Correcting the NLRP3 inflammasome deficiency in macrophages from autoimmune**  
10 **NZB mice with exon skipping antisense oligonucleotides.**

11 Sara J. Thygesen<sup>1\*</sup>, David P. Sester<sup>1\*</sup>, Simon O. Cridland<sup>1</sup>, Steve D. Wilton<sup>2,3</sup>, and Katryn J.  
12 Stacey<sup>1#</sup>

13 <sup>1</sup>School of Chemistry and Molecular Biosciences, The University of Queensland, Brisbane  
14 Qld 4072, Australia. <sup>2</sup>Western Australian Neuroscience Research Institute, Perth, Western  
15 Australia, 6009, Australia. <sup>3</sup>Centre for Comparative Genomics, Murdoch University, 90  
16 South St, Murdoch, Western Australia, 6150, Australia.

17 \*These authors contributed equally to this work

18

19

20 Running Title: Correction of *Nlrp3* splicing in NZB macrophages

21

22

23 #Corresponding author:

24 Katryn Stacey, School of Chemistry and Molecular Biosciences, The University of  
25 Queensland, Brisbane Qld 4072, Australia. Ph. +61 7 33654640. Fax +61 7 33654273.  
26 Email: katryn.stacey@uq.edu.au

27

28

29 Conflict of Interest: The authors declare no conflict of interest

30

31 **Abstract**

32 Inflammasomes are molecular complexes activated by infection and cellular stress, leading to  
33 caspase-1 activation and subsequent IL-1 $\beta$  processing and cell death. The autoimmune NZB  
34 mouse strain does not express NLRP3, a key inflammasome initiator mediating responses to a  
35 wide variety of stimuli including endogenous danger signals, environmental irritants and a  
36 range of bacterial, fungal and viral pathogens. We have previously identified an intronic point  
37 mutation in the *Nlrp3* gene from NZB mice that generates a splice acceptor site. This leads to  
38 inclusion of a pseudoexon that introduces an early termination codon and is proposed to be  
39 the cause of NLRP3 inflammasome deficiency in NZB cells. Here we have used exon  
40 skipping antisense oligonucleotides (AON) to prevent aberrant splicing of *Nlrp3* in NZB  
41 macrophages and shown that this restores both NLRP3 protein expression and NLRP3  
42 inflammasome activity. These results indicate that the single point mutation leading to  
43 aberrant splicing is the sole cause of NLRP3 inflammasome deficiency in NZB macrophages.  
44 The NZB mouse provides a novel model for addressing a splicing defect in macrophages and  
45 could be used to further investigate AON design and delivery of AONs to macrophages *in*  
46 *vivo*.

47

48

49 **Introduction**

50 Inflammasomes are multiprotein complexes that are assembled in response to microbial and  
51 endogenous danger signals and are responsible for activating caspase-1, leading to both  
52 prointerleukin (IL)-1 $\beta$  and IL-18 processing and pyroptotic cell death.<sup>1,2,3</sup> Inflammasomes  
53 can also activate apoptotic cell death through caspase-8 activation.<sup>4</sup> The best-studied  
54 inflammasome is initiated by oligomerisation of the NLRP3 protein. Many external and host-  
55 derived danger signals activate the NLRP3 inflammasome, including a range of pathogens,  
56 the bacterial ionophore nigericin, host-derived molecules such as extracellular ATP and  
57 environmental irritants including silica and asbestos.<sup>5,6,7</sup>

58

59 Recently we demonstrated that bone marrow derived macrophages (BMMs) from NZB mice  
60 are deficient in both NLRP3 and AIM2 inflammasome responses.<sup>8</sup> The NZB strain is a model  
61 of autoimmune haemolytic anaemia and systemic lupus erythematosus and develops both  
62 anti-erythrocyte and anti-nuclear antibodies.<sup>9,10</sup> Inflammasome deficiencies could alter the  
63 interaction of the host with both microflora and pathogens, promoting cytokine release  
64 favouring the development of autoimmunity.

65

66 We proposed that the NLRP3 inflammasome defect in NZB cells is due to a point mutation  
67 found in an intron that creates a splice acceptor site.<sup>8</sup> The resulting pseudoexon introduces a  
68 premature stop codon producing a less stable truncated NLRP3 protein, and an almost  
69 complete lack of NLRP3 protein expression. Here exon skipping antisense oligonucleotides  
70 (AON)<sup>11</sup> targeting the pseudoexon restored both NLRP3 protein expression and NLRP3  
71 inflammasome activity, demonstrating that this is the sole defect preventing NLRP3  
72 inflammasome function in the NZB strain.

73

74

## 75 **Results**

76 To test whether the incorporation of the pseudoexon in NZB *Nlrp3* mRNA is the sole reason  
77 for the profound NLRP3 deficiency, AONs were designed to target the pseudoexon (7b) and  
78 prevent its inclusion during pre-mRNA splicing (Figure 1A). The AONs were targeted to the  
79 splice acceptor site (AON38), splice donor site (AON40) and an intra-exonic region predicted  
80 to contain several exonic splice enhancer motifs (AON39).<sup>12,13</sup>

81

82 Preliminary experiments demonstrated that AON39, but not AON38 or AON40, was able to  
83 substantially restore NLRP3 protein expression when electroporated into NZB BMMs (data  
84 not shown). Subsequent experiments were conducted introducing AON39 or AON40 into  
85 both NZB and C57BL/6 BMMs. After 4 h, cells were primed with LPS to up-regulate  
86 NLRP3 expression. PCR of the region encompassing the pseudoexon from cDNA showed  
87 that in the absence of AON treatment the NZB *Nlrp3* mRNA was predominantly of the  
88 longer form that includes the pseudoexon (*Nlrp3'*)<sup>8</sup> while C57BL/6 samples had the correctly  
89 spliced form (Figure 1B). NZB cells treated with AON40 showed a small amount of correctly  
90 spliced mRNA, whilst AON39 restored correct splicing to the majority of the *Nlrp3* mRNA.  
91 Quantitative western blotting showed restoration of LPS-induced NLRP3 protein levels in  
92 NZB cells treated with AON39 to approximately 65% of the level in C57BL/6, while AON40  
93 was largely ineffective (Figure 1C). Without LPS priming, a small amount of NLRP3 protein  
94 was detected in NZB BMMs due to the action of AON39 on the smaller amount of nascent  
95 *Nlrp3* mRNA produced constitutively during this time.

96

97 A panel of AONs were designed to microwalk around the annealing site of AON39 in an  
98 attempt to further enhance exon skipping efficiency, with four overlapping AONs (AON80-

99 83) designed with slight target sequence and/or length variations (Figure 2A). These were  
100 introduced into NZB BMMs and changes in *Nlrp3* expression were assessed using real time  
101 PCR primers designed for either C57BL/6 *Nlrp3* mRNA, or the NZB defective *Nlrp3'*  
102 mRNA, previously validated on cloned cDNA templates. All four new AONs promoted  
103 correct splicing, and AON83 was most efficient in suppressing the aberrant *Nlrp3'* transcript  
104 and restoring the normal *Nlrp3* transcript (Figure 2B). Concomitantly, AON83 restored  
105 NLRP3 protein levels in the NZB cells to almost 80% of that in C57BL/6 cells (Figure 2C).

106

107 The longevity of the exon skipping effect of the AONs following electroporation was  
108 investigated. AON83 and AON38 (effective and ineffective treatments respectively) were  
109 electroporated into NZB and C57BL/6 BMMs. At 0, 4, 24 or 48 h post electroporation, cells  
110 were primed for 4 h with LPS and then harvested for analysis by quantitative western blot  
111 (Figure 3). Almost complete restoration of NLRP3 expression to C57BL/6 levels was  
112 observed in NZB BMMs treated with AON83 and immediately primed with LPS, but overall  
113 levels of induced NLRP3 expression in both strains were lower than later time points,  
114 probably due to electroporation-associated stress. Effective NLRP3 restoration was observed  
115 in cells left for 4 h before priming. Thereafter the effect of the AON declined with time but  
116 was still observed 48 h post treatment.

117

118 To test the effect of AON-mediated NLRP3 protein restoration on inflammasome-induced  
119 pyroptotic cell death, cell viability was measured by MTT cleavage in response to the NLRP3  
120 activator nigericin. A nigericin dose-dependent reduction in viability was seen in C57BL/6  
121 cells (Figure 4A). Untreated and AON40-treated NZB cells showed a complete lack of  
122 response but AON39 treatment restored the cell death response almost to the level of  
123 C57BL/6. Subsequently, the effect of all AONs on the response to a single, high dose of

124 nigericin was tested. The resulting inflammasome function reflected the degree of NLRP3  
125 protein restoration previously observed in cells, with AON83-treated cells the most sensitive  
126 to nigericin, showing that AON treatment can restore NLRP3 inflammasome function in  
127 NZB BMMs.

128

## 129 **Discussion**

130 Here we have used splice switching AONs to show that aberrant splicing of the *Nlrp3* gene  
131 leading to inclusion of a pseudoexon is solely responsible for the lack of NLRP3  
132 inflammasome response observed in macrophages from NZB mice. This provides proof-of-  
133 concept for restoring NLRP3 inflammasome function in NZB mice and analysing the effect  
134 on progression and severity of autoimmune disease. In addition, NZB mice could be used as a  
135 model to investigate *in vivo* delivery of AONs to macrophages.

136

137 The AONs that targeted within the pseudoexon were effective while those targeting splice  
138 acceptor and donor sites were not. Although targeting acceptor or donor sites has worked for  
139 some genes,<sup>14,15</sup> our results fit with a retrospective analysis of over 400 AONs designed for  
140 the treatment of Duchenne muscular dystrophy, that showed exon-internal AONs to be the  
141 most effective for some exons.<sup>16</sup> Other work has suggested that the proximity of the AON  
142 target site to the 5' end of the exon and the binding energetics of the oligonucleotide to the  
143 RNA are correlated with effectiveness.<sup>17</sup> Exonic splice enhancer sites promote splice site  
144 recognition and are frequently targeted by effective AONs.<sup>18</sup> Fine-tuning of the optimal AON  
145 target sequences requires experimental validation; here this was achieved by microwalking  
146 with overlapping AONs. The five overlapping exon-internal AONs had reproducible  
147 differences in their effectiveness (Figure 2). Such differences could be due to thermodynamic  
148 properties, secondary structure of the target sequence or the masking of additional exonic



149 splice enhancers. We had previously shown that longer AONs (25mers) could confer  
150 substantial improvement in exon skipping efficiency, although this requires confirmation on a  
151 case-by-case basis.<sup>19</sup>

152

153 Apart from correction of a splicing defect, exon skipping AONs can be used experimentally  
154 as an alternative to siRNA to knock down gene expression, or to induce specific splice  
155 isoforms.<sup>20</sup> A consideration for experimental use is the time course of effectiveness. Here we  
156 showed that the AONs can work very quickly and must get to the nucleus, where they  
157 hybridize with pre-mRNA,<sup>21</sup> almost immediately.

158

159 Of all disease-causing point mutations, 15% have been predicted to fall within splice sites  
160 and it has been estimated that a further 25% of confirmed pathogenic nonsense or missense  
161 mutations alter exonic splice enhancers and silencers and hence lead to abnormal splicing.<sup>22,23</sup>

162 Targeted exon skipping has potential therapeutic uses in knocking down the expression of  
163 disease causing genes or splice variants and in the restoration of normal splicing if mutations  
164 introduce deleterious pseudoexons.<sup>24</sup> Exon skipping is currently being tested in clinical trials  
165 for the treatment of Duchenne muscular dystrophy, where particular mutated exons of the  
166 dystrophin gene can be targeted to restore a correct open reading frame and protein  
167 expression.<sup>25,26</sup> Challenges that remain for exon skipping AON therapy are to define the  
168 optimal nucleic acid modifications required for stability, affinity and safety and also to  
169 optimise delivery of AONs *in vivo*. The NZB mouse provides a model for a splicing defect in  
170 macrophages, and could be used to investigate *in vivo* delivery of AONs to this compartment.

171

## 172 **2. Materials and methods**

### 173 **2.1 Materials**

174 Lipopolysaccharide (LPS) from *Salmonella minnesota* Re595 (Sigma Aldrich, St Louis,  
175 USA) was dissolved in Dulbecco's phosphate-buffered saline (PBS (Life Technologies,  
176 Grand Island, USA))/0.1% triethylamine at 10 mg/ml. Nigericin (N7143 Sigma-Aldrich) was  
177 dissolved in ethanol at 5 mM. Recombinant human CSF1 was a gift from Chiron, Emeryville,  
178 CA. Complete RPMI 1640 is RPMI 1640 with 10% heat inactivated foetal calf serum (FCS),  
179 1x GlutaMAX, 50 U/ml penicillin, 50 µg/ml streptomycin and 25 mM HEPES (all Life  
180 Technologies). MTT (3-(4,5-Dimethylthiazol-2-yl)-2,5-Diphenyltetrazolium Bromide (Life  
181 Technologies) was prepared as a 5 mg/ml stock in PBS.

182

## 183 2.2 Mice and Cell Culture

184 C57BL/6 and NZB mice were housed under specific pathogen-free conditions at the  
185 University of Queensland and were used under approval from the University of Queensland  
186 Animal Ethics Committee. Female mouse BMMs were differentiated as previously  
187 described<sup>27</sup> and used between day 7 and 10 of culture.

188

## 189 2.8 Treatment of BMMs with exon skipping oligonucleotides

190 2'-O-methyl modified AONs with a full phosphorothioate backbone were synthesized on an  
191 Expedite 8909 synthesizer using the 1micromole Thiol protocol, cleaved from the support,  
192 desalted on NAP-10 columns and stored at -20°C. AONs had the following sequences:

193 AON34-                    5'AAUAGUUUUGGCAUAAAAUUCU3';                    AON38-  
194 5'AUAUGGAAAUGUAUCUAGAUAAAUG3';                    AON39-  
195 5'CUAUGGGUUUUUGUGCUCCAAACUA3';                    AON40-  
196 5'CUUACCCAAAAGUUCUUGACUUA3',                    AON80-  
197 5'GGUUUUUGUGCUCCAAACUA3',                    AON81-5'CUAUGGGUUUUUGUGGUCCA3',

198 AON82-5'GGUUUUUGUGCUCCAAACUAUAAGU3', AON83-  
199 5'GGGUACUAUGGGUUUUUGUGCUCCA3'.

200

201 BMMs were electroporated in 400 µl of complete RPMI-1640, with or without 3.5 µM AON  
202 at 260 V, 1000 µF using a Bio-Rad Gene Pulser. Cells were immediately washed with 10 ml  
203 of complete RPMI-1640 without FCS, pelleted (350 x g, 5 min), resuspended in complete  
204 RPMI-1640 and plated out for analysis. Cells were plated for: RNA extraction at 4 million  
205 cells/well in 6-well plates, protein at 250,000-500,000 cells/well in 24-well plates and  
206 nigericin treatment/MTT assay at 70,000 cells/well in 96 well plates. Plates were incubated  
207 for 4 h and then primed with 100 ng/ml LPS for 4 h.

208

### 209 2.9 Qualitative and Real Time-quantitative PCR of *Nlrp3* variants.

210 RNA was extracted using the RNeasy mini-prep kit (Qiagen, Hilden, Germany). cDNA was  
211 generated from each sample of RNA using oligo dT priming<sup>28</sup> and amplified by conventional  
212 PCR using the forward primer 2706 (5'AGAACTGTGGTTGGTGAG3') and reverse primer  
213 3125 (5'TGTGGTTGTGGGTCAGAA3'). The products were visualised after electrophoresis  
214 on a 2% agarose gel. Quantitative real time PCR was analysed by the  $\Delta$ Ct method relative to  
215 *Hprt*, as described previously.<sup>28</sup> Primers used were NZB*Nlrp3*-For  
216 5'ATGCCTTGGGAGACTCAGGA3', NZB*Nlrp3*-Rev 5'GCTGGTGGTGGGTACTATGG3',  
217 C57*Nlrp3*-For 5'CAGAAGCTGGGGTTGGTGAAT3', C57*Nlrp3*-Rev  
218 5'CTGAGTCCTGTGTCTCCAAGG3', *Hprt*-For 5'CAGTCCCAGCGTCGTGATTAG3' and  
219 *Hprt*-Rev 5'AAACACTTTTTCCAAATCCTCGG3'.

220

### 221 2.3 Nigericin Treatment and MTT assays

222 Cells were treated with nigericin for 1 h. MTT assays of reductase activity indicating cell  
223 viability<sup>29</sup> were performed as previously described except that 5x MTT was added directly to  
224 50 µL of medium that was left in the well and was not removed prior to addition of MTT  
225 solubilisation solution (isopropanol/10% Triton X-100/0.1N HCl). Plates were left overnight  
226 for maximum solubilisation of MTT formazan product prior to measurement of absorbance at  
227 570 nm.

228

## 229 2.6 Quantitative Western Blotting

230 Cell monolayers were lysed in 100 µl 66 mM Tris pH7.4, 2% SDS. Samples were run on 15-  
231 well mini-PROTEAN TGX gels (Bio-Rad, Hercules, USA) and transferred to immobilon-FL  
232 membrane (Millipore, Billerica, USA) using a mini-trans blot system (Bio-Rad) with Tris-  
233 Glycine transfer buffer containing 10% methanol. The membrane was washed for 15 min in  
234 Tris-buffered saline (TBS) and then blocked for 1 h with Odyssey<sup>®</sup> Blocking Buffer (LI-  
235 COR, Lincoln, USA). Primary antibodies were diluted in the Odyssey<sup>®</sup> Blocking Buffer and  
236 incubated overnight at 4°C. Primary antibodies used were anti-NLRP3/NALP3 mAB, Cryo-2  
237 (#AG-20B-0014 Adipogen, San Diego, USA), anti-α-Tubulin (B-5-12, Sigma Aldrich) and  
238 anti-GAPDH (#2275-PC-020, Trevigen, Gaithersburg, USA). Membranes were washed with  
239 TBS containing 0.05% Tween-20 (TBS-T) and then incubated for 2 h, protected from light, at  
240 room temperature in secondary antibody diluted in the LI-COR buffer/0.1% Tween-20/  
241 0.01% SDS. Secondary antibodies used were anti-rabbit (Dylight) 800 conjugate, anti-rabbit  
242 (Dylight) 680 conjugate, anti-Mouse (Dylight) 800 conjugate and anti-mouse (Dylight) 680  
243 conjugate (#5151P, #5366P, #5257 and #5470P respectively, Cell Signaling Technology,  
244 Danvers, USA). Membranes were washed with TBS-T then TBS and scanned on the Odyssey  
245 (LI-COR) and analysed with Image Studio Lite software (LI-COR).

246

247 **Acknowledgements**

248 KJS was supported by a National Health and Medical Research Council (NHMRC)  
249 Fellowship 1059729 and work was supported by NHMRC grant 1050651.

250

251 **Conflicts of Interest**

252 The authors declare no conflict of interest.

253

254 **References**

255 1. Martinon F, Burns K, Tschopp J. The inflammasome: a molecular platform triggering  
256 activation of inflammatory caspases and processing of proIL-beta. *Mol Cell* 2002;  
257 **10(2)**: 417-26.

258

259 2. Ghayur T, Banerjee S, Hugunin M, Butler D, Herzog L, Carter A *et al.* Caspase-1  
260 processes IFN-gamma-inducing factor and regulates LPS-induced IFN-gamma  
261 production. *Nature* 1997; **386(6625)**: 619-23.

262

263 3. Thornberry NA, Bull HG, Calaycay JR, Chapman KT, Howard AD, Kostura MJ *et al.*  
264 A novel heterodimeric cysteine protease is required for interleukin-1 beta processing  
265 in monocytes. *Nature* 1992; **356(6372)**: 768-74.

266

- 267 4. Sagulenko V, Thygesen SJ, Sester DP, Idris A, Cridland JA, Vajjhala PR *et al.* AIM2  
268 and NLRP3 inflammasomes activate both apoptotic and pyroptotic death pathways  
269 via ASC. *Cell Death Differ* 2013; **20**(9): 1149-60.
- 270
- 271 5. Bauernfeind F, Hornung V. Of inflammasomes and pathogens--sensing of microbes  
272 by the inflammasome. *EMBO Mol Med* 2013; **5**(6): 814-26.
- 273
- 274 6. Mariathasan S, Weiss DS, Newton K, McBride J, O'Rourke K, Roose-Girma M *et al.*  
275 Cryopyrin activates the inflammasome in response to toxins and ATP. *Nature* 2006;  
276 **440**(7081): 228-32.
- 277
- 278 7. Dostert C, Petrilli V, Van Bruggen R, Steele C, Mossman BT, Tschopp J. Innate  
279 immune activation through Nalp3 inflammasome sensing of asbestos and silica.  
280 *Science* 2008; **320**(5876): 674-7.
- 281
- 282 8. Sester DP, Sagulenko V, Thygesen SJ, Cridland JA, Loi YS, Cridland SO *et al.*  
283 Deficient NLRP3 and AIM2 Inflammasome Function in Autoimmune NZB Mice. *J*  
284 *Immunol* 2015; **195**(3): 1233-41.
- 285
- 286 9. Scatizzi JC, Haraldsson MK, Pollard KM, Theofilopoulos AN, Kono DH. The Lbw2  
287 locus promotes autoimmune hemolytic anemia. *J Immunol* 2012; **188**(7): 3307-14.

288

- 289 10. Borchers A, Ansari AA, Hsu T, Kono DH, Gershwin ME. The pathogenesis of  
290 autoimmunity in New Zealand mice. *Semin Arthritis Rheum* 2000; **29**(6): 385-99.
- 291
- 292 11. Aartsma-Rus A, van Ommen GJ. Antisense-mediated exon skipping: a versatile tool  
293 with therapeutic and research applications. *RNA* 2007; **13**(10): 1609-24.
- 294
- 295 12. Fairbrother WG, Yeh RF, Sharp PA, Burge CB. Predictive identification of exonic  
296 splicing enhancers in human genes. *Science* 2002; **297**(5583): 1007-13.
- 297
- 298 13. Yeo G, Hoon S, Venkatesh B, Burge CB. Variation in sequence and organization of  
299 splicing regulatory elements in vertebrate genes. *Proc Natl Acad Sci USA* 2004;  
300 **101**(44): 15700-5.
- 301
- 302 14. Gallego-Villar L, Viecelli HM, Perez B, Harding CO, Ugarte M, Thony B *et al.* A  
303 sensitive assay system to test antisense oligonucleotides for splice suppression therapy  
304 in the mouse liver. *Mol Ther Nucleic Acids* 2014; **3**: e193.
- 305
- 306 15. Karras JG, McKay RA, Dean NM, Monia BP. Deletion of individual exons and  
307 induction of soluble murine interleukin-5 receptor-alpha chain expression through  
308 antisense oligonucleotide-mediated redirection of pre-mRNA splicing. *Mol*  
309 *Pharmacol* 2000; **58**(2): 380-7.

310

- 311 16. Aartsma-Rus A, Houlleberghs H, van Deutekom JC, van Ommen GJ, t Hoen PA.  
312 Exonic sequences provide better targets for antisense oligonucleotides than splice site  
313 sequences in the modulation of Duchenne muscular dystrophy splicing.  
314 *Oligonucleotides* 2010; **20**(2): 69-77.
- 315
- 316 17. Echigoya Y, Mouly V, Garcia L, Yokota T, Duddy W. In silico screening based on  
317 predictive algorithms as a design tool for exon skipping oligonucleotides in Duchenne  
318 muscular dystrophy. *PloS One* 2015; **10**(3): e0120058.
- 319
- 320 18. Aartsma-Rus A, van Vliet L, Hirschi M, Janson AA, Heemskerk H, de Winter CL *et*  
321 *al.* Guidelines for antisense oligonucleotide design and insight into splice-modulating  
322 mechanisms. *Mol Ther* 2009; **17**(3): 548-53.
- 323
- 324 19. Harding PL, Fall AM, Honeyman K, Fletcher S, Wilton SD. The influence of  
325 antisense oligonucleotide length on dystrophin exon skipping. *Mol Ther* 2007; **15**(1):  
326 157-66.
- 327
- 328 20. Fletcher S, Adams AM, Johnsen RD, Greer K, Moulton HM, Wilton SD. Dystrophin  
329 isoform induction in vivo by antisense-mediated alternative splicing. *Mol Ther* 2010;  
330 **18**(6): 1218-23.
- 331
- 332 21. Sazani P, Kole R. Therapeutic potential of antisense oligonucleotides as modulators  
333 of alternative splicing. *J Clin Invest* 2003; **112**(4): 481-6.



334

335 22. Krawczak M, Reiss J, Cooper DN. The mutational spectrum of single base-pair  
336 substitutions in mRNA splice junctions of human genes: causes and consequences.  
337 *Hum Genet* 1992; **90**(1-2): 41-54.

338

339 23. Sterne-Weiler T, Howard J, Mort M, Cooper DN, Sanford JR. Loss of exon identity is  
340 a common mechanism of human inherited disease. *Genome Res* 2011; **21**(10): 1563-  
341 71.

342

343 24. Veltrop M, Aartsma-Rus A. Antisense-mediated exon skipping: taking advantage of a  
344 trick from Mother Nature to treat rare genetic diseases. *Exp Cell Res* 2014; **325**(1):  
345 50-5.

346

347 25. Koo T, Wood MJ. Clinical trials using antisense oligonucleotides in duchenne  
348 muscular dystrophy. *Hum Gene Ther* 2013; **24**(5): 479-88.

349

350 26. Cirak S, Arechavala-Gomez V, Guglieri M, Feng L, Torelli S, Anthony K *et al.*  
351 Exon skipping and dystrophin restoration in patients with Duchenne muscular  
352 dystrophy after systemic phosphorodiamidate morpholino oligomer treatment: an  
353 open-label, phase 2, dose-escalation study. *Lancet* 2011; **378**(9791): 595-605.

354

- 355 27. Sester DP, Brion K, Trieu A, Goodridge HS, Roberts TL, Dunn J *et al.* CpG DNA  
356 activates survival in murine macrophages through TLR9 and the phosphatidylinositol  
357 3-kinase-Akt pathway. *J Immunol* 2006; **177**(7): 4473-80.
- 358
- 359 28. Cridland JA, Curley EZ, Wykes MN, Schroder K, Sweet MJ, Roberts TL *et al.* The  
360 mammalian PYHIN gene family: phylogeny, evolution and expression. *BMC Evol*  
361 *Biol* 2012; **12**: 140.
- 362
- 363 29. Berridge MV, Tan AS. Characterization of the cellular reduction of 3-(4,5-  
364 dimethylthiazol-2-yl)-2,5-diphenyltetrazolium bromide (MTT): subcellular  
365 localization, substrate dependence, and involvement of mitochondrial electron  
366 transport in MTT reduction. *Arch Biochem Biophys* 1993; **303**(2): 474-82.
- 367
- 368
- 369
- 370
- 371

372 **Figure Legends**

373 **Figure 1. Antisense oligonucleotide treatment can restore normal splicing and NLRP3**  
374 **expression in NZB cells. (A)** Diagram showing the *Nlrp3* pseudoexon 7b, the location of the  
375 point mutation (triangle) and the position of the AONs. AON38 anneals to the last 11bp  
376 upstream of the pseudoexon and the first 14 bases of the pseudoexon. AON39 anneals  
377 entirely within the pseudoexon targeting nucleotides 21 to 46 from the 5' end. AON40  
378 anneals to the last 20 nucleotides of the pseudoexon and the first 5 nucleotides of the  
379 downstream intron. **(B)** AON39 restores the normal *Nlrp3* mRNA splicing within NZB  
380 BMMs. BMMs from NZB and C57BL/6 mice were electroporated with AON39 or AON40  
381 or with no addition, incubated for 4 h, then primed with 100 ng/ml LPS for 4 h. Conventional  
382 PCR using primers in exons 6/7 and 9, flanking the pseudoexon 7b, shows the mRNA  
383 variants with the pseudoexon (*Nlrp3'*) or without the pseudoexon (*Nlrp3*) in NZB and  
384 C57BL/6 BMMs after AON treatment. **(C)** AON39 restores NLRP3 protein levels in NZB  
385 BMMs. Quantitative western blot of NLRP3 protein levels normalised to tubulin expression,  
386 from cells treated as in panel B, with and without LPS priming.

387 **Figure 2. Refinement of optimal AON targeting sequence. (A)** Diagram showing the  
388 position of four additional AON relative to AON39. AON80, 81, 82 and 83 all anneal within  
389 the pseudoexon, targeting nucleotides 21-40, 26-45, 16-40 and 26-50 from the 5' end  
390 respectively. A predicted exonic splice enhancer motif is shown in white text. **(B)** Effects of  
391 minor sequence changes to AON on *Nlrp3* splicing, assessed by quantitative PCR. BMMs  
392 from NZB or C57BL/6 mice were electroporated with either no addition (-), a control  
393 oligonucleotide (cont), or an AON (38-40, 80-83), incubated for 4 h, then primed with 100  
394 ng/ml LPS for 4 h. Quantitative real time PCR analysis was performed with primers specific  
395 for *Nlrp3'* (with pseudoexon) and *Nlrp3* (correct splicing). Data were normalised to NZB  
396 without oligonucleotide for *Nlrp3'* results and C57BL/6 without oligonucleotide for *Nlrp3*

397 results and show the mean and range from two experiments. **(C)** Effects of minor sequence  
398 changes to AON on NLRP3 protein expression, assessed by quantitative western blotting.  
399 NLRP3 protein levels from cells treated as in panel B were assessed relative to GAPDH  
400 expression. Data shown is the mean and range of two experiments, normalised to the  
401 C57BL/6 without AON sample.

402 **Figure 3. Exon skipping AON have diminishing potency during the 48 h post**  
403 **introduction into cells.** BMMs from NZB and C57BL/6 mice were electroporated with no  
404 addition (-), AON38 or AON83, plated and primed with 100 ng/ml LPS for 4 h, immediately  
405 (0h) or after 4, 24 or 48 h of incubation. A quantitative western blot is shown for NLRP3  
406 protein levels normalised to GAPDH. As samples within each experiment were analysed on  
407 two separate blots, 0h and 4h sample data is shown relative to 4h C57BL/6 without  
408 oligonucleotide and 24h and 48h sample data is shown relative to 48h C57BL/6 without  
409 oligonucleotide. Quantitative data shown is the mean and range of two experiments.

410 **Figure 4. Inhibition of aberrant splicing restores NLRP3 inflammasome function in**  
411 **NZB BMMs.** Relative cell viability was measured by MTT cleavage. **(A)** NZB and C57BL/6  
412 BMMs were electroporated with nothing (-), AON40 or AON39, incubated for 4 h and then  
413 primed with 100 ng/ml LPS for 4 h. NLRP3 inflammasome was triggered by treatment with  
414 0, 1.25, 2.5, 5 or 10  $\mu$ M nigericin for 1 h. Data represent the mean and standard deviation of  
415 triplicate nigericin treatments of each AON-electroporated sample. Results are relative to the  
416 mean of the 0  $\mu$ M nigericin wells for each sample, and are representative of three  
417 experiments performed. **(B)** NZB and C57BL/6 BMMs were electroporated with nothing (-),  
418 control oligonucleotide (cont), or the indicated AON, incubated for 4 h and then primed with  
419 100 ng/ml LPS for 4 h. Cells were then treated with or without 10  $\mu$ M nigericin for 1 h. Cell  
420 viability is shown relative to the unstimulated cells for each oligonucleotide treatment. Data

421 is representative of two experiments and shows the mean and standard deviation of triplicate  
422 treatments from one experiment.

423

Figure 1

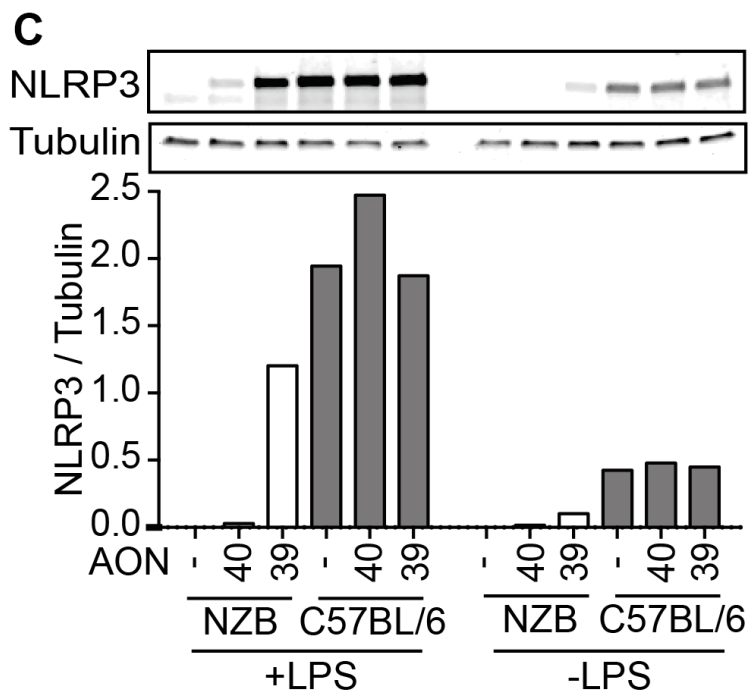
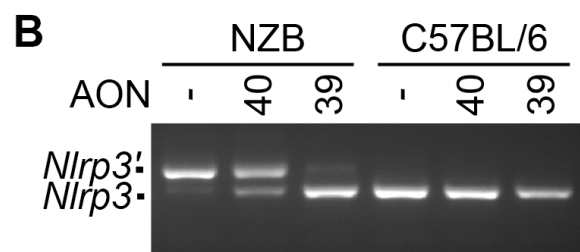
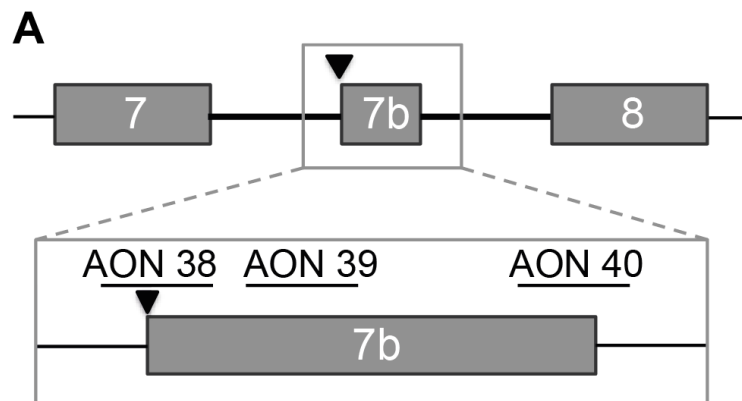


Figure 2

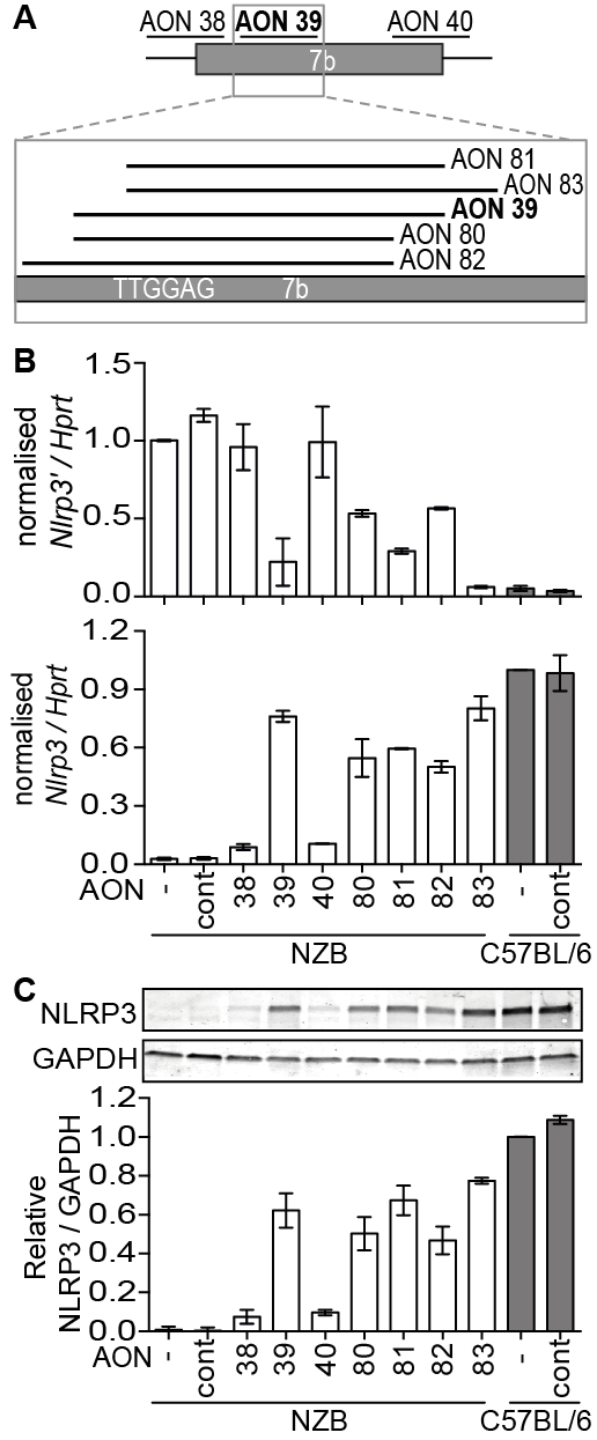


Figure 3

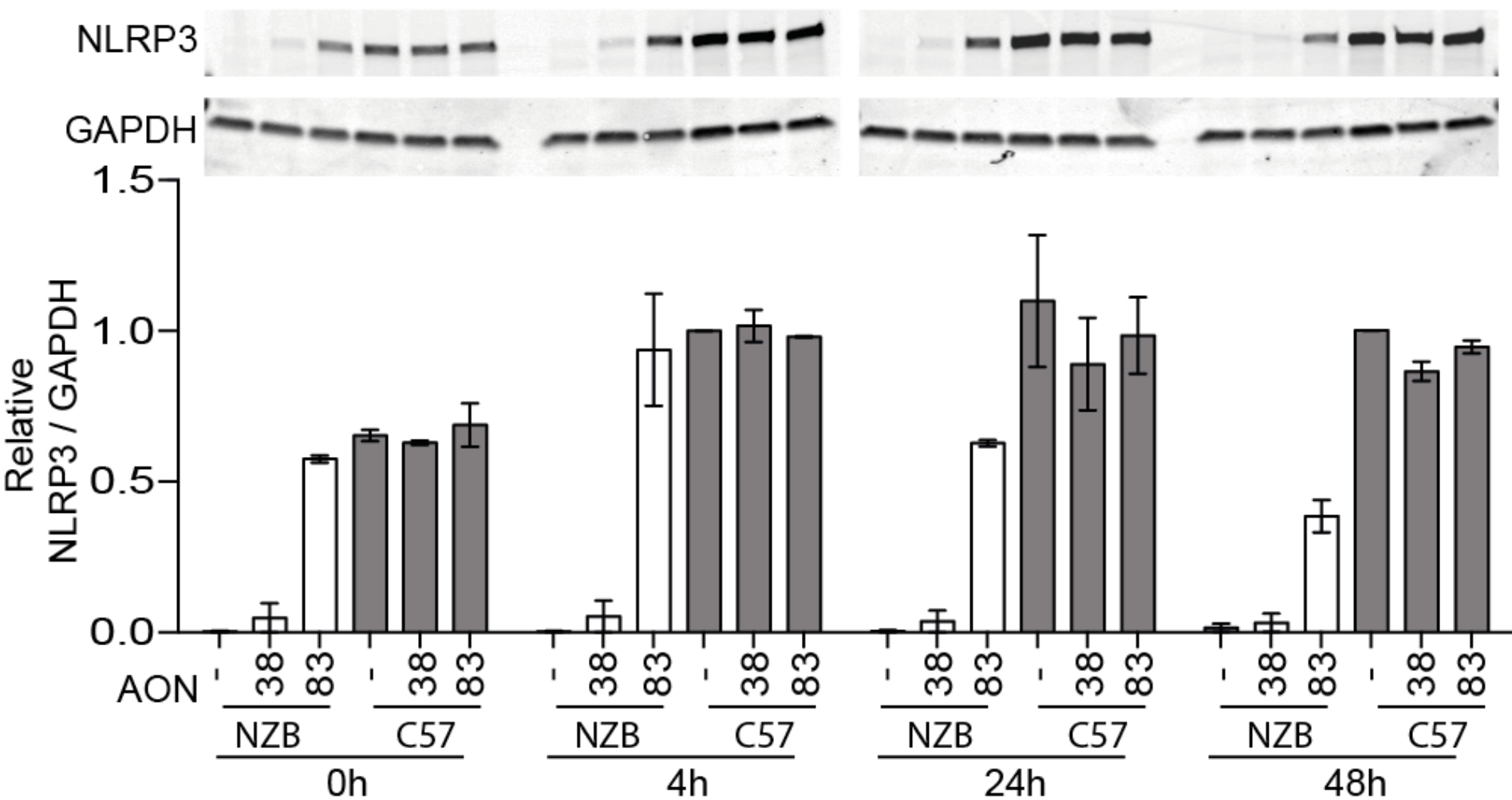




Figure 4

